

Reversible Data Hiding Algorithm Based on Pixel Value Ordering and Edge Detection Mechanism

Thai-Son Nguyen*, Hoang-Nam Tram, and Phuoc-Hung Vo

School of Engineering and Technology, Tra Vinh University

Tra Vinh Province, Viet Nam

[e-mail: thaison@tvu.edu.vn, tramhoangnam@tvu.edu.vn, hungvo@tvu.edu.vn]

*Corresponding author: Thai-Son Nguyen

*Received April 22, 2022; accepted October 1, 2022;
published October 31, 2022*

Abstract

Reversible data hiding is an algorithm that has ability to extract the secret data and to restore the marked image to its original version after data extracting. However, some previous schemes offered the low image quality of marked images. To solve this shortcoming, a new reversible data hiding scheme based on pixel value ordering and edge detection mechanism is proposed. In our proposed scheme, the edge image is constructed to divide all pixels into the smooth regions and rough regions. Then, the pixels in the smooth regions are separated into non overlapping blocks. Then, by taking advantages of the high correlation of current pixels and their adjacent pixels in the smooth regions, PVO algorithm is applied for embedding secret data to maintain the minimum distortion. The experimental results showed that our proposed scheme obtained the larger embedding capacity. Moreover, the greater image quality of marked images are achieved by the proposed scheme than that other previous schemes while the high EC is embedded.

Keywords: PVO, high image quality, reversible data hiding, prediction error, edge detection.

1. Introduction

Reversible data hiding is an algorithm that has ability to extract the secret data. Moreover, in RDH schemes, the cover images can be completely restored after extracting the embedded secret data. The main reason is that their original version of the cover images plays significant role in different fields, i.e., medical, military, and law forensics images. Therefore, any smallest modifications in these images are not allowed. As a result, RDH schemes have interested a lot of researchers. In the last two decades, several RDH schemes that are proposed and can be mainly partitioned into two different categories i.e., difference expansion (DE) [1]–[8] and histogram shifting (HS) [9]–[24]. In the DE-based RDH scheme, J. Tian [1] first proposed in 2003. For embedding data, Tian calculated the difference value of two adjacent pixels and expanded it to conceal one secret bit. To maintain the correctly data extracting and the completely reconstructing of the original image, a location map is required for tracking the position of embedded pixels. However, the EC of Tian's scheme is low, around 0.15 bits per pixel (bpp). The main reason is that in their scheme only one secret bit is embedded into a pair of pixels while the location map is required to be reversibility. Later on, A. Alattar [2] improved the performance of Tian's scheme, n of pixels are applied for embedding $n-1$ of secret bits. Therefore, the EC of Alattar's scheme is slightly improved when the average of EC is 0.19 bpp. However, the image quality is limited when the PSNR of the embedded image is always smaller than 45 dB. To increase the EC, Kim et al. [3] minimized the size of the location map for a RDH scheme by using the Laplace distribution. In the HS-based RDH scheme, Ni et al. [9] first constructed a histogram of the occurrence frequency of pixels for RDH algorithm in 2006. Then, to extract the secret bits correctly and restore the original image completely, in such histogram, a pair of peak and zero points are determined to carry the secret data. In 2009, Sachnev et al. [10] proposed a novel HS-based RDH technique. In Sachnev et al.'s scheme, to determine smooth pixels for carrying the secret data, all image pixels are sorted in ascending order of the local variance values to increases the height of peak bin. Therefore, their embedding capacity is significantly improved. In 2013, Li et al. [11] combined of pixel value ordering (PVO) and prediction-error expansion for HS-based RDH scheme. The original image is partitioned into non-overlapping blocks in Li et al.'s scheme. Then, the pixels with the highest and lowest values in each block are predicted for data hiding. In the PVO scheme, prediction errors with value of 1 and -1 are used to carry the secret bits. However, their embedding capacity is low, approximate 0.1 bpp. To solve the shortcoming in Li et al.'s scheme, Peng et al. [12] proposed improved PVO scheme (IPVO) by utilizing both prediction errors with value of 0 and 1 for embedding secret data. Their scheme obtained the higher EC while guaranteeing the high visual quality of marked images. To improve the quality of the marked images further, Qu et al. [13] proposed new HS-based RDH scheme (PPVO) by predicting the value of a current pixel according to its adjacent pixels in each block. Then, the prediction value is modified for embedding the secret information. Years later, to improve the EC further, Meikap et al. [15] proposed a clever RDH scheme based on a generalized directional PVO (DPVO) with block size varied. In the DPVO scheme, cover image is partitioned into blocks which are enlarged by using image interpolation mechanism. Then, overlapped embedding in three different directions of each block is applied to achieve the high embedding capacity. In 2018, Vo et al. [17] proposed a novel RDH technique based on two-dimensional histogram shifting to improve the EC and image quality. Later on, to increase the EC, Lee et al. [22] proposed generalized PVO (GePVO) by using a reference pixel. In their scheme, the reference pixel, the middle pixel of the block, is used to calculate prediction errors for two sides of the block. Their scheme achieved the high EC when the large size of image

block is used. However, the PSNR of the marked images is significantly reduced. To improve the EC while maintaining the high visual quality of marked images, in this paper, a new PVO-based RDH scheme is proposed. In our scheme, edge detection algorithm is utilized to categorize pixels into the smooth or rough regions. Then, taking advantage of the high pixel redundancy in the smooth regions, such pixels in block are sorted in ascending order and the middle pixel is used as a reference pixel to calculate the prediction errors for embedding data. Experimental results have demonstrated that the proposed scheme achieves higher visual quality of marked images than that of the existing schemes while guaranteeing the high embedding capacity.

The remainder of the paper is structured as following: some related works are described in Section 2. Then, Section 3 presents our proposed scheme. The experimental results are presented in Section 4. Then, conclusions are drawn in Section 5.

2. Related Works

In 2013, Li et al. introduced PVO mechanism for RDH technique. In this scheme, the cover image is separated into non overlapping blocks B_i with the size of $n \times m$. Then, the block B_i is converted to vector $X_i = \{x_1, x_2, \dots, x_{n \times m}\}$ and arranged in the ascending order to get vector $B_\sigma = \{x_{\sigma(1)}, x_{\sigma(2)}, \dots, x_{\sigma(n \times m)}\}$. Then, the difference values are calculated by (1).

$$\begin{cases} PE_{max} = x_{\sigma(n \times m)} - x_{\sigma(n \times m - 1)} \\ PE_{min} = x_{\sigma(1)} - x_{\sigma(2)} \end{cases} \quad (1)$$

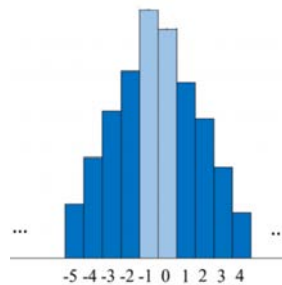


Fig. 1. An example of prediction error's histogram

A histogram of prediction errors is formed as shown in **Fig. 1**. The prediction errors are modified by (2) and (3) for embedding where $b = \{0,1\}$ is secret bit.

$$PE'_{max} = \begin{cases} PE'_{max} + b & \text{if } PE_{max} = 1 \\ PE'_{max} + 1 & \text{if } PE_{max} > 1' \end{cases} \quad (2)$$

$$PE'_{min} = \begin{cases} PE'_{min} - b & \text{if } PE_{min} = -1 \\ PE'_{min} - 1 & \text{if } PE_{min} < -1' \end{cases} \quad (3)$$

Then, only the prediction errors with the value of $PE_{max} = 1$ and $PE_{min} = -1$ are used to contain the secret bits. As a result, their EC is limited by the height of $PE_{max} = 1$ and $PE_{min} = -1$.

To improve the EC further, Lee et al. proposed GePVO scheme. In their scheme, various non-overlapping block sizes, the reference pixel is determined for prediction. Then, the block with the size of $n_1 \times n_2$ is reordered in the ascending order to form vector $B_\sigma = \{p_{\sigma(1)}, p_{\sigma(2)}, \dots, p_{\sigma(n_1 \times n_2)}\}$. Next, the non- positive and non-negative prediction errors, dp_i and dn_i , are calculated by (4) where $p_{\sigma(g)}$ is the reference pixel and $g = \lceil \frac{n_1 \times n_2}{2} \rceil$.

$$\begin{cases} dp_i = p_{\sigma(n_1 \times n_2 - i + 1)} - p_{\sigma(n_1 \times n_2 - i)}, \\ (i = 1, 2, \dots, n_1 \times n_2 - g), dn_i = p_{\sigma(i)} - p_{\sigma(i+1)}, i = 1, 2, \dots, g - 1 \end{cases} \quad (4)$$

The histogram of prediction errors is constructed and used for embedding data. Assuming that two bins, i.e., pk^+ and pk^- , are the highest frequency ones in the histogram. The prediction errors dp_i and dn_i are modified to embed data according to (5) and (6).

$$dp'_i = \begin{cases} dp_i + s & \text{if } dp_i = pk^+ \\ dp_i + 1 & \text{if } dp_i > pk^+ \end{cases} \quad (5)$$

$$dn'_i = \begin{cases} dn_i - s & \text{if } dn_i = pk^- \\ dn_i - 1 & \text{if } dn_i > pk^- \end{cases} \quad (6)$$

Lee et al.'s scheme obtained the high EC value. However, once the large sizes of the block are used, it leads to constructing the large prediction errors in the block. Thus, the visual image quality of the marked images is significantly reduced when carrying on the secret information. To deal with this shortcoming, we proposed a novel PVO-based RDH scheme. To ensure minimum modification during embedding process, the cover image is separated into the smooth and rough regions by applying one of the well-known edge detection mechanisms. Then, take the advantage of the high correlation of the current pixels and their adjacent pixels, the smooth regions are partitioned into the adaptive blocks for embedding data. The goal of this change guarantees the modification of prediction errors as small as possible. As a result, the proposed method obtained greater image quality while maintaining high embedding capacity.

3. Proposed Scheme

In this section, to increase the image quality of the marked images while maintaining high EC, the cover image is classified as either complex or smooth regions by using edge detection mechanisms. To ensure the minimum distortion, the complex regions are kept unchanged during the embedding procedure. This is because the complex regions usually provide less embedding capacity than the smooth blocks. However, they always offer larger distortion than smooth regions when carrying the secret data.

Instead of using the various sizes of block with rectangle shape to embed secret data as done in Lee et al. [22]. In our proposed scheme, a different manner of block partition is used to exploit the high correlation of adjacent pixels in the smooth regions. In particular, to guarantee the high quality of marked images, the original image is subsequently separated into two block types with the size of three pixels, i.e., Type-A and Type-B, as illustrated in Fig. 2. For each block, the pixels are sorted in the ascending order. Then, the difference values of the highest pixel and the lowest pixels are calculated to conceal the secret bits. The detailed description is presented in the following subsections, including, pre-processing, data embedding, and data extracting phases.

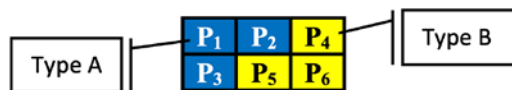
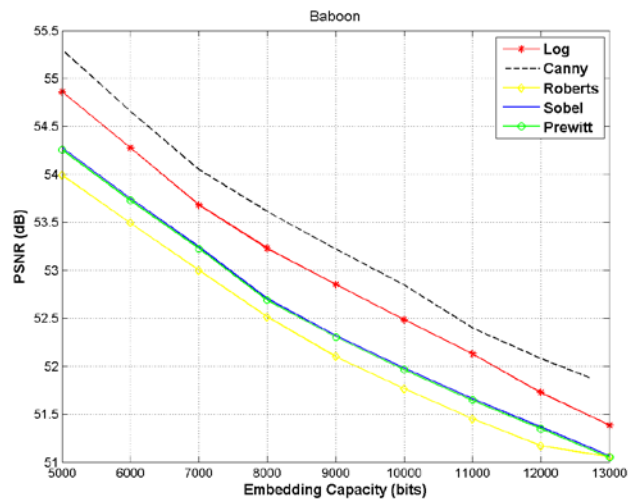


Fig. 2. Block partition

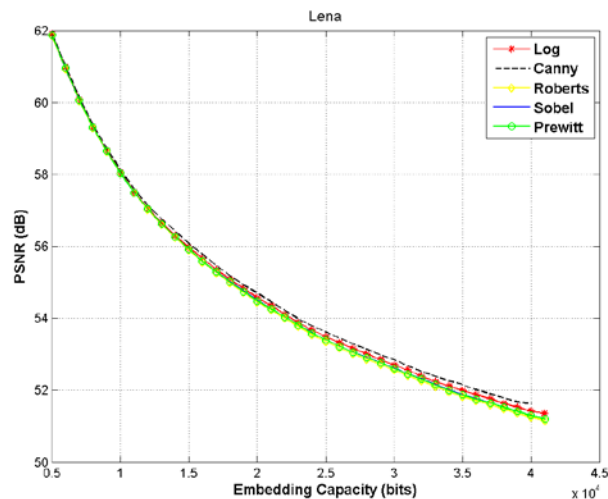
3.1 Image pre-processing

In this subsection, to classify pixels into the smooth or rough regions, one of well-known edge detection mechanisms is used. Traditionally, the edge image is calculated from the original

version of cover images by utilizing the edge detector algorithm. However, in our scheme, ensuring the same edge image is obtained during the embedding process, the last three least-significant-bit (3-LSBs) of all pixels are cleared to generate the most-significant-bit (MSB) image I_{MSB} . Then, the image I_{MSB} is used to calculate the edge image I_{edge} , to guarantee low extra information. In order to extract data correctly, in the data extracting phase, the same edge image is reconstructed from the MSB marked image. In the proposed scheme, the modification is only occurred in the last 3-LSBs while the 5-MSBs of all pixels kept unchanged during embedding process. Therefore, the same edge image is obtained for extracting data.



3(a)



3(b)

Fig. 3. Compare the PSNR of five edge detection algorithms 3(a) Lena, 3(b) Baboon

To guarantee the trade-off between the visual quality and the EC, some well-known edge detection approaches, i.e., sobel, prewitt, roberts, log, canny techniques are analyzed for the proposed scheme. **Fig. 3** showed that the visual quality and the EC value for the images “Lena” and “Baboon”. It is obvious that the proposed scheme with Canny edge detection (CED) mechanism achieves the better performance than with other edge detection mechanisms.

Therefore, in the proposed scheme, CED is performed in the image I_{MSB} to construct the edge image I_{edge} . Then, according to I_{edge} , the image I is partitioned into smooth or complex regions. All pixels of the smooth region are employed to embed data by using PVO algorithm. For the rough regions, all pixels are prevented from any modification during the embedding process.

3.2 Data embedding procedure

In our scheme, the pixel value may be altered by 1 unit for embedding. Therefore, pixels with the values of 0 or 255 might be altered to -1 and 256 after embedding procedure, causing the overflow/underflow problems. To overcome this shortcoming, the positions of the pixels with the values of 0 or 255 are recorded into the location map LM . Then, such pixel values are changed to 1 or 254, respectively. To preserve more room for embedding data, the LM is compressed by arithmetic coding algorithm. To ensure reversibility, the extra information, including the compressed LM and the side information, should be obtained before extracting data in the data extraction procedure. The flowchart of our proposed embedding technique is shown in Fig. 4.

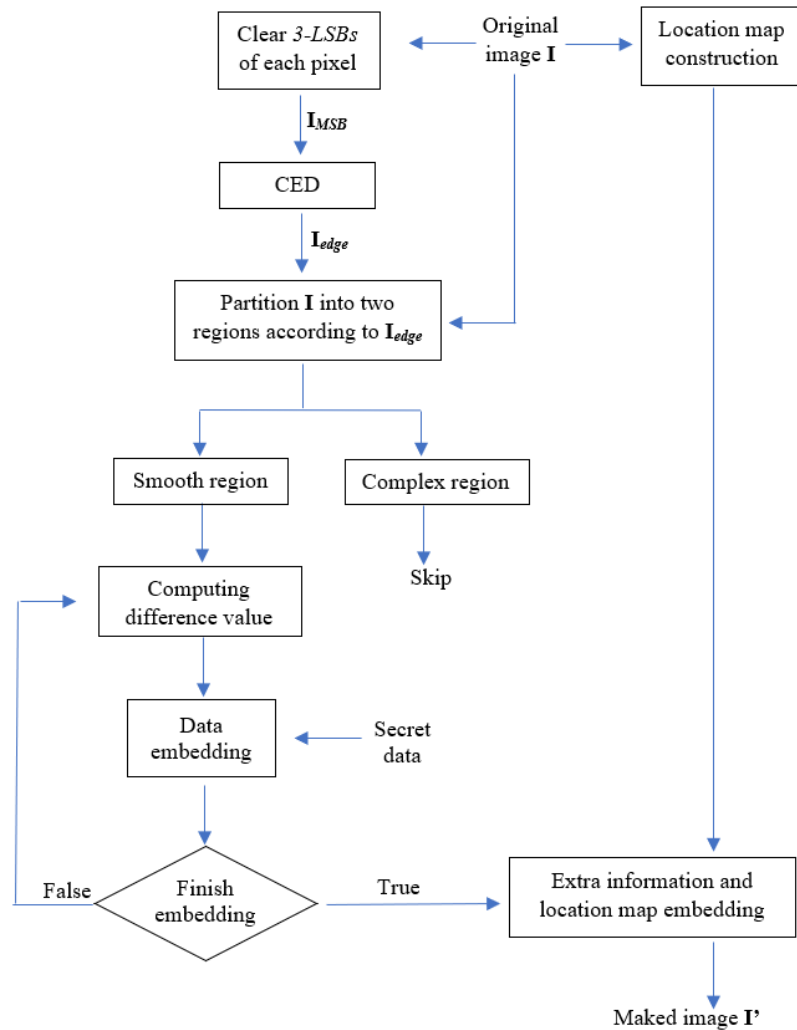


Fig. 4. Flowchart of embedding algorithm

+ Input: The original image I with the size of $n \times m$ and the secret data B .

+ Output: The marked image I' .

Step 1: Remove 3-LSBs bits of all pixels in I to obtain I_{MSB} . Then, perform CED algorithm on the image I_{MSB} to generate the edge image I_{edge} .

Step 2: Record the position of pixels with the values of 0 or 255 by LM and compressed by arithmetic coding algorithm.

Step 3: According to I_{edge} , partition the pixels in the smooth regions into non-overlap blocks as shown in Fig. 2.

Step 4: With each block, pixels were arranged in ascending order to get a vector $P = \{p_{\pi(1)}, p_{\pi(2)}, p_{\pi(3)}\}$ where $p_{\pi(1)} \leq p_{\pi(2)} \leq p_{\pi(3)}$.

Step 5: The pixel $p_{\pi(2)}$ is then used as the reference pixel to predict for the pixel $p_{\pi(1)}$ and $p_{\pi(3)}$. The largest prediction error d_{max} and smallest prediction error d_{min} are computed by (7), (8)

$$d_{max} = \begin{cases} p_{\pi(3)} - p_{\pi(2)} & \text{if } \pi(2) > \pi(3) \\ p_{\pi(2)} - p_{\pi(3)} & \text{otherwise} \end{cases}, \quad (7)$$

$$d_{min} = \begin{cases} p_{\pi(2)} - p_{\pi(1)} & \text{if } \pi(1) > \pi(2) \\ p_{\pi(1)} - p_{\pi(2)} & \text{otherwise} \end{cases}. \quad (8)$$

Step 6: Then, d_{max} and d_{min} are used to construct the histogram. If $d_{max} = 0$ or $d_{max} = 1$, they are used to embed the data. Otherwise, d_{max} will be shifted toward to the right 1 unit. Then, the corresponding pixels are calculated by (9).

$$p'_{\pi(3)} = \begin{cases} p'_{\pi(3)} + b & \text{if } d_{max} = 0 \text{ or } d_{max} = 1 \\ p'_{\pi(3)} + 1 & \text{if } d_{max} < 0 \text{ or } d_{max} > 1 \end{cases}. \quad (9)$$

Likewise, if $d_{min} = 0$ or $d_{min} = 1$, they are also used for embedding data. Otherwise, d_{min} are shifted toward to the left 1 unit. The marked pixels are calculated by (10).

$$p'_{\pi(1)} = \begin{cases} p'_{\pi(1)} - b & \text{if } d_{min} = 0 \text{ or } d_{min} = 1 \\ p'_{\pi(1)} - 1 & \text{if } d_{min} < 0 \text{ or } d_{min} > 1 \end{cases}. \quad (10)$$

Repeat the Steps 5 and 6 till all of the secrets information are hidden, record the coordinate of the last embedding pixel P_{end} .

Step 7: Embedding extra information: Extract the LSB of first $2 \cdot \log_2(n \times m)$ pixels in the last row of the image I to obtain the binary sequence S_{LSB} . Next, replace LSB of those pixels by extra information, including the location map ($\log_2(n \times m)$ bits), P_{end} ($\log_2 n + \log_2 m$ bits) to guarantee reversibility. Then, the binary sequence S_{LSB} are embedded to I from the pixel P_{end+1} to generate the marked image I' .

3.3 Data extracting procedure

Since obtaining the marked image I' from the sender, the receiver can extract the secret data and reconstruct the original image as followings:

+ Input: The marked image I' .

+ Output: The secret data B and the cover image I .

Step 1: Remove 3-LSBs bits of all marked pixels. Then, the CED is applied to construct the edge image I_{edge} for classifying smooth or complex regions.

Step 2: Extract extra information from LSB of first $2 \cdot \log_2(n \times m)$ pixels in the last rows of the marked image. Then, reconstruct the location map, the last position P_{end} .

Step 3: According to I_{edge} , all marked pixels in the smooth regions of I' are separated into non-overlap blocks as **Fig. 2**.

Step 4: With each block, pixels were arranged in ascending order to get vector $P' = \{p'_{\pi(1)}, p'_{\pi(2)}, p'_{\pi(3)}\}$.

Step 5: Then, $p'_{\pi(2)}$ is used as the reference pixel to predict for $p'_{\pi(1)}$ and $p'_{\pi(3)}$. The largest (and smallest) prediction error d'_{max} (and d'_{min}) are calculated by (11) and (12).

$$d'_{max} = \begin{cases} p'_{\pi(3)} - p'_{\pi(2)} & \text{if } \pi(2) > \pi(3) \\ p'_{\pi(2)} - p'_{\pi(3)} & \text{otherwise} \end{cases}, \quad (11)$$

$$d'_{min} = \begin{cases} p'_{\pi(2)} - p'_{\pi(1)} & \text{if } \pi(1) > \pi(2) \\ p'_{\pi(1)} - p'_{\pi(2)} & \text{otherwise} \end{cases}. \quad (12)$$

Step 6: According to d'_{max} and d'_{min} the secret bits are extracted by (13) and (14).

$$b = \begin{cases} d'_{max} - 1 & \text{if } d'_{max} \in \{1, 2\} \\ -d'_{max} & \text{if } d'_{max} \in \{0, -1\} \end{cases} \quad (13)$$

$$b = \begin{cases} d'_{min} - 1 & \text{if } d'_{min} \in \{1, 2\} \\ -d'_{min} & \text{if } d'_{min} \in \{0, -1\} \end{cases}. \quad (14)$$

Then, the value of the original pixels is restored by (15) and (16), respectively.

$$p''_{\pi(3)} = \begin{cases} p'_{\pi(3)} - b & \text{if } d'_{max} \in \{-1, 0, 1, 2\} \\ p'_{\pi(3)} - 1 & \text{if } d'_{max} < 0 \text{ or } d'_{max} > 2 \end{cases} \quad (15)$$

$$p''_{\pi(1)} = \begin{cases} p'_{\pi(1)} - b & \text{if } d'_{min} \in \{-1, 0, 1, 2\} \\ p'_{\pi(1)} - 1 & \text{if } d'_{min} < 0 \text{ or } d'_{min} > 2 \end{cases}. \quad (16)$$

Repeat the Steps 5 and 6 until the last embedding pixel P_{end} is reached, all secret bits have been extracted. Then, extract the sequence S_{LSB} from the pixel P_{end+1} by using Steps 5 and 6. Finally, the *LSB* of first $2 \cdot \log_2(n \times m)$ pixels in the last rows of I' are replaced by the sequence S_{LSB} to generate I'' .

Step 7: According to the location map, the cover image I is reconstructed completely.

4. Experimental Results

In this section, to evaluate the performance of the proposed scheme, nine standards 512×512 grayscale images with varying complexity characteristics are used as test images, as shown in **Fig. 5**. In the experiment, two following criteria are used to compare the performance of the proposed scheme and that of existing schemes [10], [12], [22]:

- Embedding capacity (EC): The criterion is used to evaluate how many of secret bits can be embedded into the cover image.
- Peak signal-to-noise ratio (PSNR): The criterion is used to determine the visual quality of the marked images. The higher PSNR is, the better quality of marked images is obtained.

The PSNR is calculate by (17), where MSE denotes as the average squared difference between original and marked images is calculate by (18). $C(r, c)$ and $S(r, c)$ are the original pixel and the marked pixel values in the row r and the column c , respectively.

$$PSNR = 10 \cdot \log_{10} \left(\frac{255^2}{MSE} \right), \quad (17)$$

$$MSE = \frac{1}{r \cdot c} \sum_{r=0}^{r-1} \sum_{c=0}^{c-1} [C(r, c) - S(r, c)]^2. \quad (18)$$

In addition, our proposed scheme is compared to three other existing schemes: PVO, IPVO, GePVO. In this experiment, to ensure fair comparison, the GePVO scheme in two different

block sizes, i.e., the size of 1×4 (GePVO 1×4) and the size of 1×5 (GePVO 1×5), is used. **Fig. 6** presents the comparison in terms of PSNR at the different EC. This comparison was shown by a line chart, that began with the EC at 5000 bits and continued to its highest. Where a step size of 5000 bits is used. As shown in **Fig. 6**, the top curve is our proposed scheme. As was the case for EC value, the image quality of our scheme was superior to the other three schemes (PVO, IPVO, GePVO). Our PSNR always is higher than 60 dB in the most of images when the EC is 5000 bits. Except Baboon, the complex image, the PSNR of this image is maintained higher than 54 dB. In **Fig. 6**, it is obvious that the proposed scheme always provides the better performance. Since PVO, IPVO, GePVO schemes use the large size of blocks for embedding data, that causes larger prediction errors are generated. Therefore, the quality of marked images is significantly reduced. In our scheme, by taking advantage of the correlation of the pixel and its adjacent pixels, the small block size is used to obtain the smaller prediction errors. Moreover, CED is also used to prevent any modification of pixels in the complex regions where always generate the large prediction errors. As a result, our scheme outperforms previous schemes in terms of the visual quality.

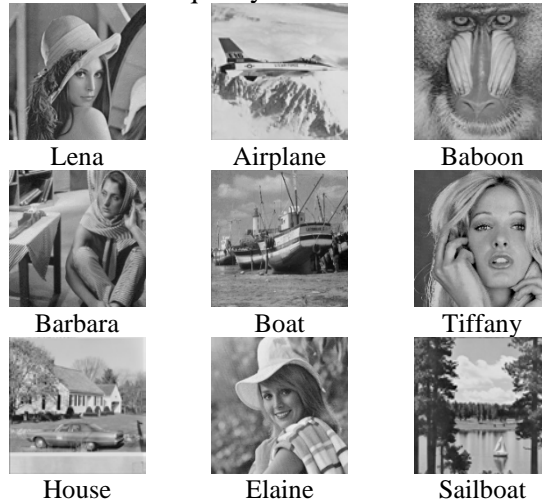


Fig. 5. Test image used in the experiments

Table 1. Comparison of PSNR (dB) between the proposed scheme and PVO, IPVO, GePVO schemes for EC of 10,000 bits

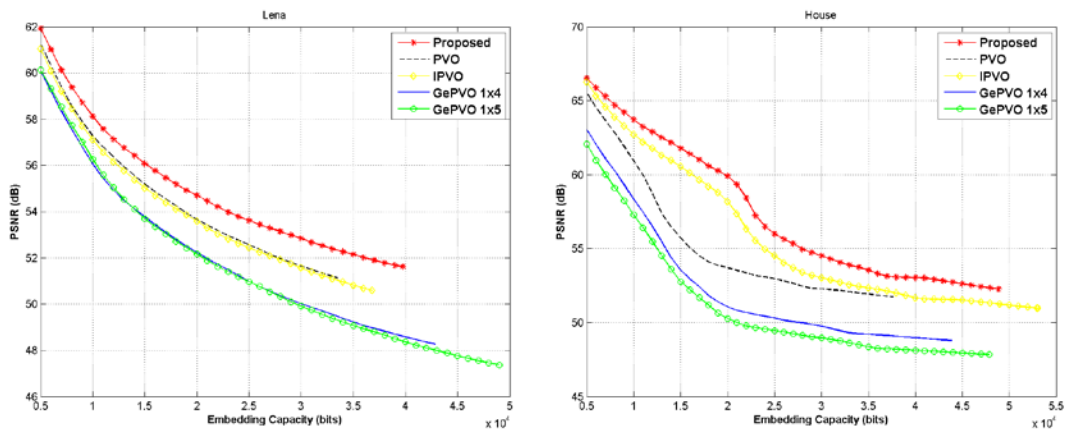
Image	Proposed	PVO [10]	IPVO [12]	GePVO 1×4 [22]	GePVO 1×5 [22]
Lena	58.13	57.28	57.11	56.07	56.27
Airplane	58.88	59.06	58.61	57.53	57.24
Baboon	52.49	51.71	51.66	49.43	48.94
Barbara	57.67	56.45	56.33	54.23	53.63
Boat	59.97	60.25	59.75	59.60	59.83
Tiffany	57.87	57.25	57.07	55.64	55.53
House	63.73	60.95	62.72	58.36	57.29
Sailboat	56.85	55.91	55.80	54.00	53.64
Elaine	55.81	54.82	55.49	53.41	53.25
Average	57.93	57.08	57.17	55.36	55.07

The proposed scheme is compared to PVO, IPVO, and GePVO in **Table 1**. When the EC of 10,000 bits is used, our PSNR values are slightly increased. Since, the PSNR is higher than that of existing schemes, about 0.86 dB, 0.76 and 2.57 dB on average, respectively. In **Table 2**, when the larger secret amount is embedded, the proposed scheme has improved the results obtained by previous schemes significantly. In GePVO, Lee et al.'s scheme used various sizes of the block for embedding data. However, only the pixel in middle of the block is used as reference pixel to ensure reversibility. As a result, their approach only maintained high image quality when the EC was low. In contrast, to minimize distortion of the marked images by using the small block size, and carefully picking the smooth regions with CED mechanism are combined for embedding data.

Table 2. Comparison of PSNR (dB) between the proposed scheme and PVO, IPVO, GePVO schemes for EC of 20,000 bits

Image	Proposed	PVO [10]	IPVO [12]	GePVO 1x4 [22]	GePVO 1x5 [22]
Lena	54.70	53.65	53.59	52.23	52.16
Airplane	56.26	56.60	56.01	55.07	54.84
Barbara	53.63	51.84	52.14	50.47	50.17
Boat	56.68	56.12	56.06	55.55	55.71
Tiffany	54.98	54.05	53.90	52.39	52.34
House	59.91	53.71	58.19	51.06	50.28
Sailboat	53.26	52.26	52.42	51.10	50.88
Elaine	52.11	51.50	51.65	49.75	49.68
Average	55.19	53.72	54.25	52.20	52.01

Table 2 illustrates the results for 20,000 bits embedding capacity. In **Table 2**, the higher quality of marked images are obtained by the proposed scheme among four schemes. Once the average PSNR gained by proposed scheme over PVO, IPVO, GePVO are 1.47 dB, 0.94 dB and 2.99 dB, respectively. The proposed scheme is based on CED mechanism. then, only the blocks in the smooth regions are utilized to embed data while keeping all pixels in complex regions of the cover images unchanged in the data embedding process. As a result, the high virtual quality of marked images is maintained.



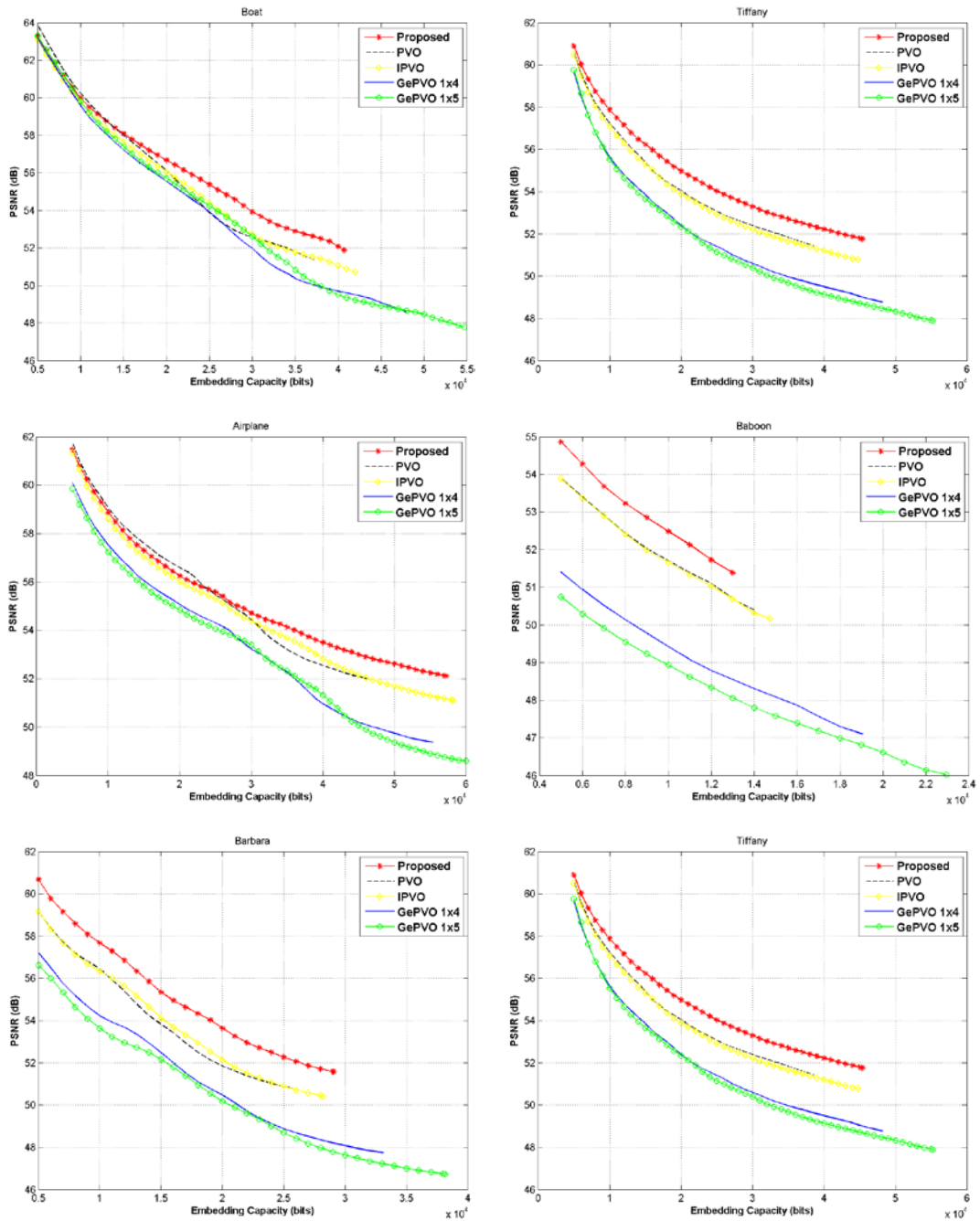


Fig. 6. Comparing the performance of proposed scheme with PVO, IPVO, GePVO

5. Conclusion

In this work, a new RDH scheme based on pixel value ordering technique and edge detection mechanism. To obtain the high image quality, in the proposed scheme, the Canny edge detection algorithm is employed to categorize the image blocks into smooth or rough regions. Then, to guarantee the high image quality of marked images, only for smooth regions, the

secret data are embedded into by modifying small value of the pixels. According to the experimental results, in comparison with the existing schemes, the proposed RDH scheme provides the better image quality for marked images while maintaining the high embedding capacity.

References

- [1] Jun Tian, "Reversible data embedding using a difference expansion," *IEEE Trans. Circuits Syst. Video Technol.*, vol. 13, no. 8, pp. 890-896, Aug. 2003. [Article \(CrossRef Link\)](#)
- [2] A. M. Alattar, "Reversible Watermark Using the Difference Expansion of a Generalized Integer Transform," *IEEE Trans. Image Process.*, vol. 13, no. 8, pp. 1147-1156, Aug. 2004. [Article \(CrossRef Link\)](#)
- [3] Hyoung Joong Kim, V. Sachnev, Yun Qing Shi, Jeho Nam, and Hyon-Gon Choo, "A Novel Difference Expansion Transform for Reversible Data Embedding," *IEEE Trans. Inf. Forensics Secur.*, vol. 3, no. 3, pp. 456-465, Sep. 2008. [Article \(CrossRef Link\)](#)
- [4] Y. Hu, H.-K. Lee, K. Chen, and J. Li, "Difference Expansion Based Reversible Data Hiding Using Two Embedding Directions," *IEEE Trans. Multimed.*, vol. 10, no. 8, pp. 1500-1512, Dec. 2008. [Article \(CrossRef Link\)](#)
- [5] Yongjian Hu, Heung-Kyu Lee, and Jianwei Li, "DE-Based Reversible Data Hiding With Improved Overflow Location Map," *IEEE Trans. Circuits Syst. Video Technol.*, vol. 19, no. 2, pp. 250-260, Feb. 2009. [Article \(CrossRef Link\)](#)
- [6] Xiaolong Li, Weiming Zhang, Xinlu Gui, and Bin Yang, "A Novel Reversible Data Hiding Scheme Based on Two-Dimensional Difference-Histogram Modification," *IEEE Trans. Inf. Forensics Secur.*, vol. 8, no. 7, pp. 1091-1100, Jul. 2013. [Article \(CrossRef Link\)](#)
- [7] C.-F. Lee, J.-J. Shen, Y.-J. Wu, and S. Agrawal, "Reversible Data Hiding Scheme Based on Difference Expansion Using Shiftable Block Strategy for Enhancing Image Fidelity," in *2019 IEEE 10th International Conference on Awareness Science and Technology (iCAST)*, Morioka, Japan, pp. 1-6, Oct. 2019. [Article \(CrossRef Link\)](#)
- [8] T.-S. Nguyen and P.-H. Vo, "Reversible image authentication scheme based on prediction error expansion," *Indones. J. Electr. Eng. Comput. Sci.*, vol. 21, no. 1, pp. 253-262, Jan. 2021. [Article \(CrossRef Link\)](#)
- [9] Zhicheng Ni, Yun-Qing Shi, N. Ansari, and Wei Su, "Reversible data hiding," *IEEE Trans. Circuits Syst. Video Technol.*, vol. 16, no. 3, pp. 354-362, Mar. 2006. [Article \(CrossRef Link\)](#)
- [10] V. Sachnev, Hyoung Joong Kim, Jeho Nam, S. Suresh, and Yun Qing Shi, "Reversible Watermarking Algorithm Using Sorting and Prediction," *IEEE Trans. Circuits Syst. Video Technol.*, vol. 19, no. 7, pp. 989-999, Jul. 2009. [Article \(CrossRef Link\)](#)
- [11] X. Li, J. Li, B. Li, and B. Yang, "High-fidelity reversible data hiding scheme based on pixel-value-ordering and prediction-error expansion," *Signal Process.*, vol. 93, no. 1, pp. 198-205, Jan. 2013. [Article \(CrossRef Link\)](#)
- [12] F. Peng, X. Li, and B. Yang, "Improved PVO-based reversible data hiding," *Digit. Signal Process.*, vol. 25, pp. 255-265, Feb. 2014. [Article \(CrossRef Link\)](#)
- [13] X. Qu and H. J. Kim, "Pixel-based pixel value ordering predictor for high-fidelity reversible data hiding," *Signal Process.*, vol. 111, pp. 249-260, Jun. 2015. [Article \(CrossRef Link\)](#)
- [14] G. Xuan, X. Li, and Y.-Q. Shi, "Histogram-pair based reversible data hiding via searching for optimal four thresholds," *J. Inf. Secur. Appl.*, vol. 39, pp. 58-67, Apr. 2018. [Article \(CrossRef Link\)](#)
- [15] S. Meikap and B. Jana, "Directional PVO for reversible data hiding scheme with image interpolation," *Multimed. Tools Appl.*, vol. 77, no. 23, pp. 31281-31311, Dec. 2018. [Article \(CrossRef Link\)](#)
- [16] T.-S. Nguyen, C.-C. Chang, and T.-H. Shih, "Effective reversible image steganography based on rhombus prediction and local complexity," *Multimed. Tools Appl.*, vol. 77, no. 20, pp. 26449-26467, Oct. 2018. [Article \(CrossRef Link\)](#)

- [17] P.-H. Vo, T.-S. Nguyen, V.-T. Huynh, and T.-N. Do, "A novel reversible data hiding scheme with two-dimensional histogram shifting mechanism," *Multimed. Tools Appl.*, vol. 77, no. 21, pp. 28777–28797, Nov. 2018. [Article \(CrossRef Link\)](#)
- [18] F. Di, M. Zhang, X. Liao, and J. Liu, "High-fidelity reversible data hiding by Quadtree-based pixel value ordering," *Multimed. Tools Appl.*, vol. 78, no. 6, pp. 7125–7141, Mar. 2019. [Article \(CrossRef Link\)](#)
- [19] F. Di, M. Zhang, F. Huang, J. Liu, and Y. Kong, "Reversible data hiding in JPEG images based on zero coefficients and distortion cost function," *Multimed. Tools Appl.*, vol. 78, no. 24, pp. 34541–34561, Dec. 2019. [Article \(CrossRef Link\)](#)
- [20] C.-F. Lee, J.-J. Shen, Y.-J. Wu, and S. Agrawal, "PVO-Based Reversible Data Hiding Exploiting Two-Layer Embedding for Enhancing Image Fidelity," *Symmetry*, vol. 12, no. 7, Art. no. 7, Jul. 2020. [Article \(CrossRef Link\)](#)
- [21] W. Wang and W. Wang, "New High Capacity Reversible Data Hiding Using the Second-Order Difference Shifting," *IEEE Access*, vol. 8, pp. 85367–85379, 2020. [Article \(CrossRef Link\)](#)
- [22] C.-F. Lee, J.-J. Shen, S. Agrawal, Y.-J. Tseng, and Y.-C. Kao, "A generalized pixel value ordering data hiding with adaptive embedding capability," *J. Supercomput.*, vol. 76, no. 4, pp. 2683–2714, Apr. 2020. [Article \(CrossRef Link\)](#)
- [23] W. He and Z. Cai, "An Insight into Pixel Value Ordering Prediction Based Prediction-error Expansion," *IEEE Trans. Inf. Forensics Secur.*, pp. 3859–3871, 2020. [Article \(CrossRef Link\)](#)
- [24] T.-S. N. Thai-Son Nguyen, C.-C. C. Thai-Son Nguyen, and Chin-Chen Chang, "High Capacity Reversible Data Hiding Scheme based on AMBTC for Encrypted Images," *Journal of Internet Technology*, vol. 23, no. 2, pp. 255–266, Mar. 2022. [Article \(CrossRef Link\)](#)



Thai-Son Nguyen received the M.S. and Ph.D. degrees from Feng Chia University, Taichung, Taiwan, in 2011 and 2015, respectively, all in computer science. He has served as a lecturer in Tra Vinh University, Vietnam, from 2006. From 2019, he was Dean of the school of Engineering and Technology, Tra Vinh University. He is currently an Associate professor. His research interests include image processing, information hiding, image recognition, information security, IoT and artificial intelligence applications. Dr. Son has served a member of Editorial board for Scientific Journal of Tra Vinh University and Journal of Science, Engineering and Technology.



Hoang-Nam Tram was received the bachelor's degree Mathematics and Informatics from Can Tho University, Can Tho City, in 2009 and the master's degree in Computer Science from the University of Information Technology – Vietnam National University Ho Chi Minh City in 2015. He has worked as a lecturer in the School of Engineering and Technology, Tra Vinh University since 2009. His areas of interest include data hiding, information security, image and signal processing.



Phuoc-Hung Vo received the B.S. degree in information technology from Can Tho University, Can Tho City, Vietnam, in 1996. From October 1996 he has been lecturer of Tra Vinh Continuous Training Center, Tra Vinh Community College and then Tra Vinh University. He received M. Sc degree in Computer science from Feng Chia University, Taiwan, in 2011, and Ph.D. degree in Information system from Can Tho University in 2021. His current research interests are multimedia security and image processing.